Three-dimensional Imaging of Pion using Lattice QCD: Generalized Parton Distributions

Qi Shi

BNL & CCNU

Based on arXiv: 2407.03516

In collaboration with H.-T. Ding, X. Gao, S. Mukherjee, P. Petreczky, S. Syritsyn and Y. Zhao

Introduction: GPDs

1D

Form Factor (pion-electron scattering)

Parton Distribution Functions (Drell-Yan process)

} Generalized Parton Distributions

3D

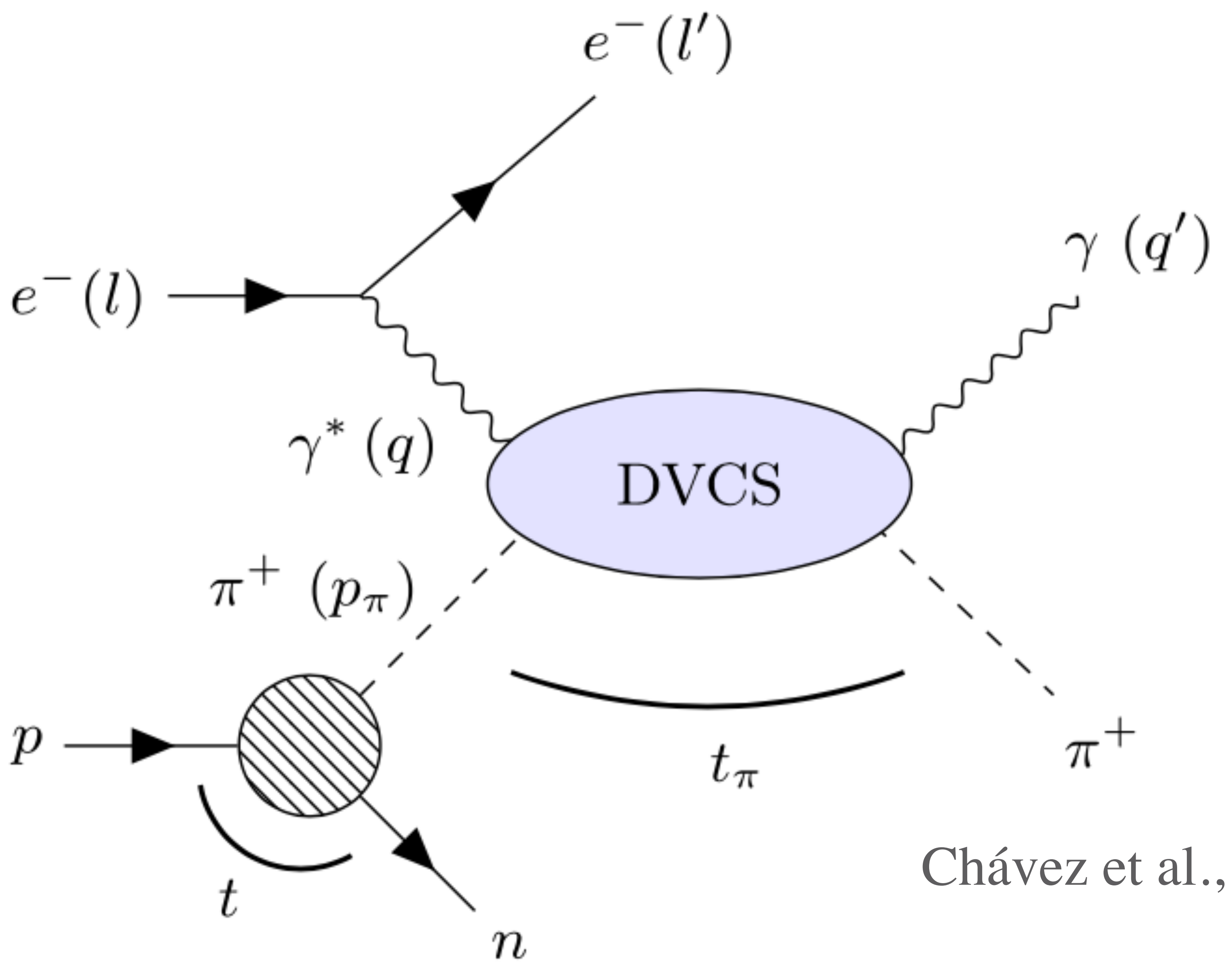

Chávez et al., PRL 128 (2022) 202501

+ **Models**

Lattice QCD: from first principle

Frame-independent approach

- **Traditional: Symmetric (Breit)**

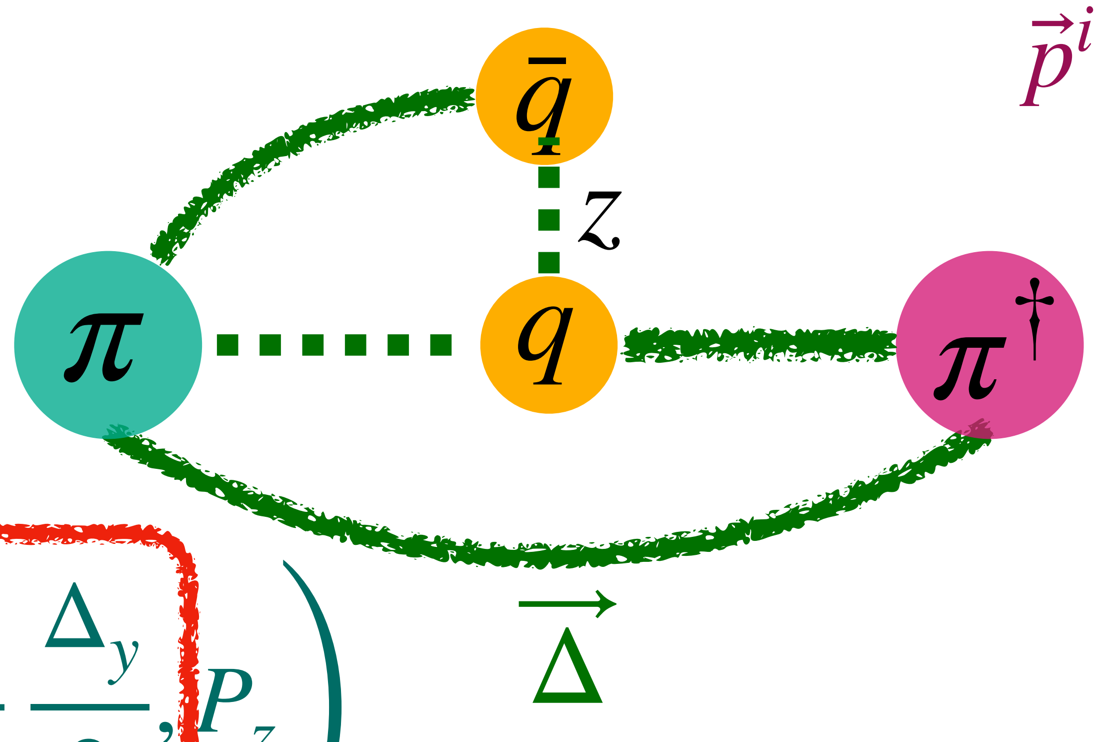

$\vec{p}^{\,i} = \bar{P} - \frac{\vec{\Delta}}{2} = \left(-\frac{\Delta_x}{2}, -\frac{\Delta_y}{2}, P_z\right)$

$\vec{p}^{\,f} = \bar{P} + \frac{\vec{\Delta}}{2} = \left(+\frac{\Delta_x}{2}, +\frac{\Delta_y}{2}, P_z\right)$

- Fix $\vec{p}^{\,f}$ — only one t is useful

- **Newly proposed: Asymmetric (non-Breit)**

Bhattacharya et al., PRD 106 (2022) 114512

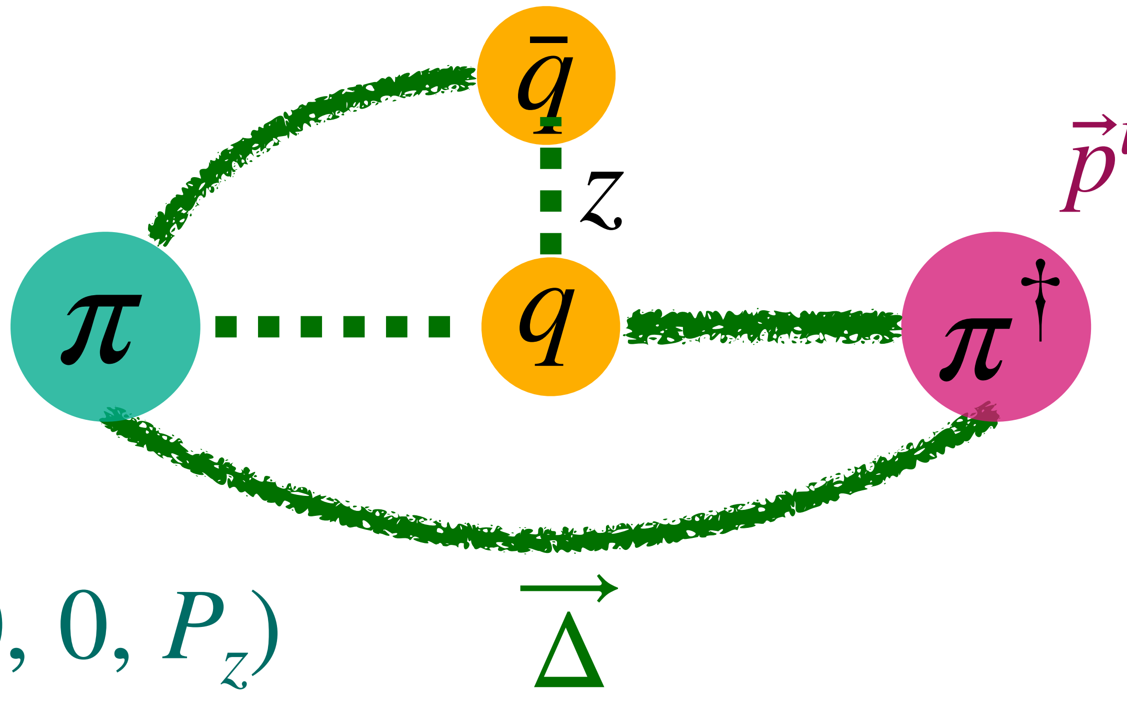

$\vec{p}^{\,i} = \vec{p}^{\,f} - \vec{\Delta} = (-\Delta_x, \Delta_y, P_z)$

$\vec{p}^{\,f} = (0, 0, P_z)$

- Fix $\vec{p}^{\,f}$ — several t are useful

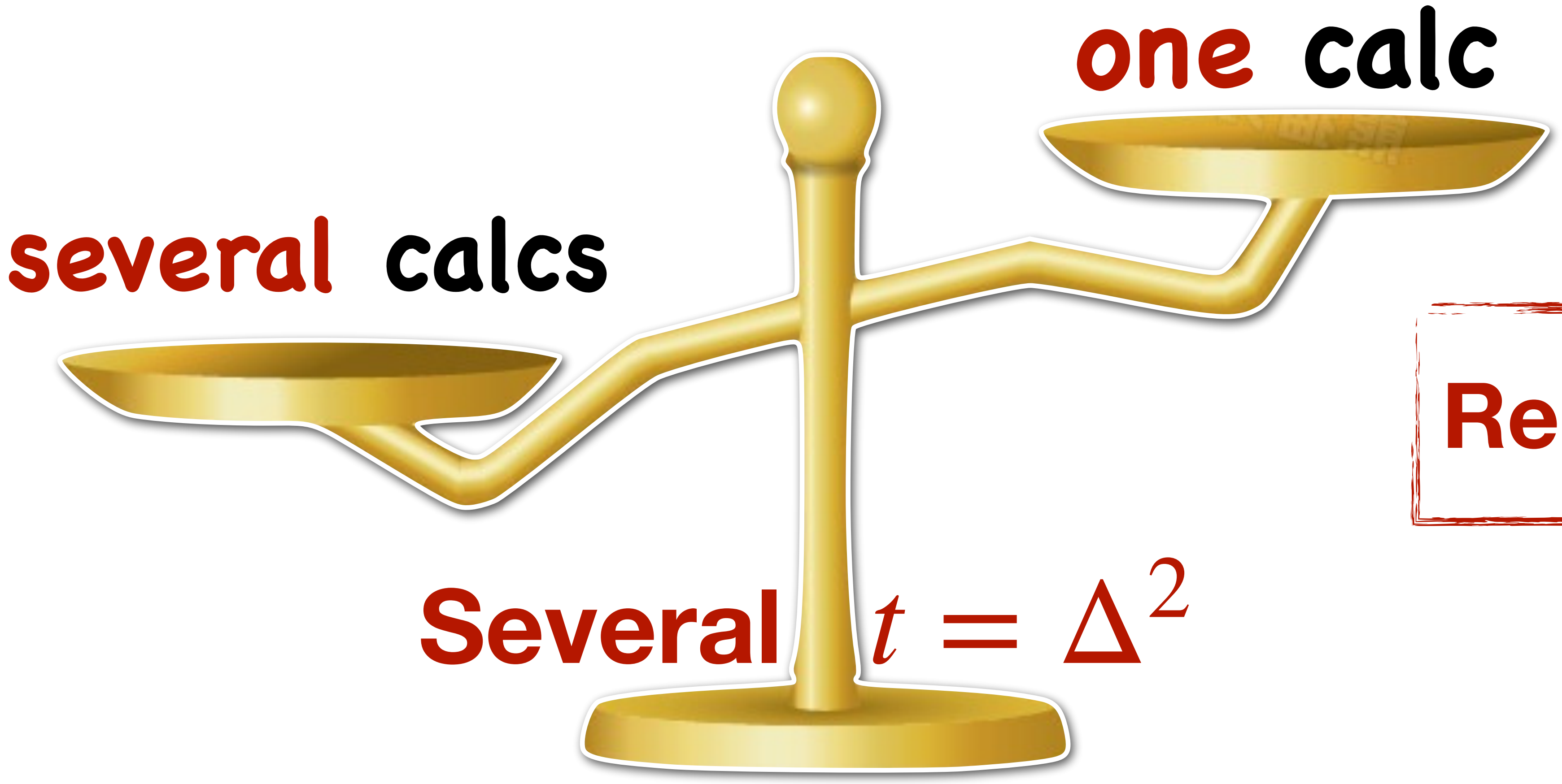

Huge computational cost

Reduced computational cost

Frame-independent approach

- Matrix elements

$$M^\mu(z,\bar{P},\Delta) = \left\langle \pi(P^f) \,|\, O^{\gamma_\mu}(z) \,|\, \pi(P^i) \right\rangle, \qquad O^{\gamma_\mu}(z) = \frac{1}{2}\left[\bar{u}(-\frac{z}{2})\gamma^\mu \mathscr{W}_{-\frac{z}{2},\frac{z}{2}} u(\frac{z}{2}) - \bar{d}(-\frac{z}{2})\gamma^\mu \mathscr{W}_{-\frac{z}{2},\frac{z}{2}} d(\frac{z}{2})\right].$$

- Lorentz-invariant amplitudes A_i's

$$M^\mu(z,\bar{P},\Delta) = \bar{P}^\mu A_1 + m_\pi^2 z^\mu A_2 + \Delta^\mu A_3, \qquad \bar{P}^\mu = (p_f^\mu + p_i^\mu)/2, \quad \Delta^\mu = p_f^\mu - p_i^\mu .$$

- Lorentz-invariant quasi-GPD $\widetilde{H}_{\mathrm{LI}}$

$$\widetilde{H}_{\mathrm{LI}}(z\cdot\bar{P}, z\cdot\Delta, \Delta^2 = t, z^2) \equiv A_1(z\cdot\bar{P}, z\cdot\Delta, \Delta^2, z^2) + \frac{z\cdot\Delta}{z\cdot\bar{P}} A_3(z\cdot\bar{P}, z\cdot\Delta, \Delta^2, z^2)$$

$$\widetilde{H}(x,\xi,t) = \int \frac{d(z\cdot\bar{P})}{2\pi} e^{ixz\cdot\bar{P}} \widetilde{H}_{\mathrm{LI}}(z\cdot\bar{P}, z\cdot\Delta, t, z^2)$$

- LaMET Ji, PRL 110 (2013) 262002

$$H(x,\mu,t) = \int_{-\infty}^{\infty} \frac{\mathrm{d}k}{|k|} \int_{-\infty}^{\infty} \frac{\mathrm{d}y}{|y|} \mathscr{C}_{\mathrm{evo}}^{-1}\left(\frac{x}{k}, \frac{\mu}{\mu_0}\right) \mathscr{C}^{-1}\left(\frac{k}{y}, \frac{\mu_0}{yP_z}, |y|\lambda_s\right) \widetilde{H}(y, P_z, t, z_s, \mu_0)$$

Lorentz-invariant Amplitudes

In principle

- A_i (Breit) $\sim A_i$ (Non-Breit)
- $A_3(-z \cdot \Delta) = -A_3(z \cdot \Delta)$

$\xrightarrow{\xi = 0} A_3(z \cdot \Delta = 0) = 0$

In practice

$P_z = 0.968$ GeV^2,

$$-t = \begin{cases} 0.938 \text{ GeV}^2, & \text{Breit} \\ 0.952 \text{ GeV}^2, & \text{Non-breit} \end{cases}$$

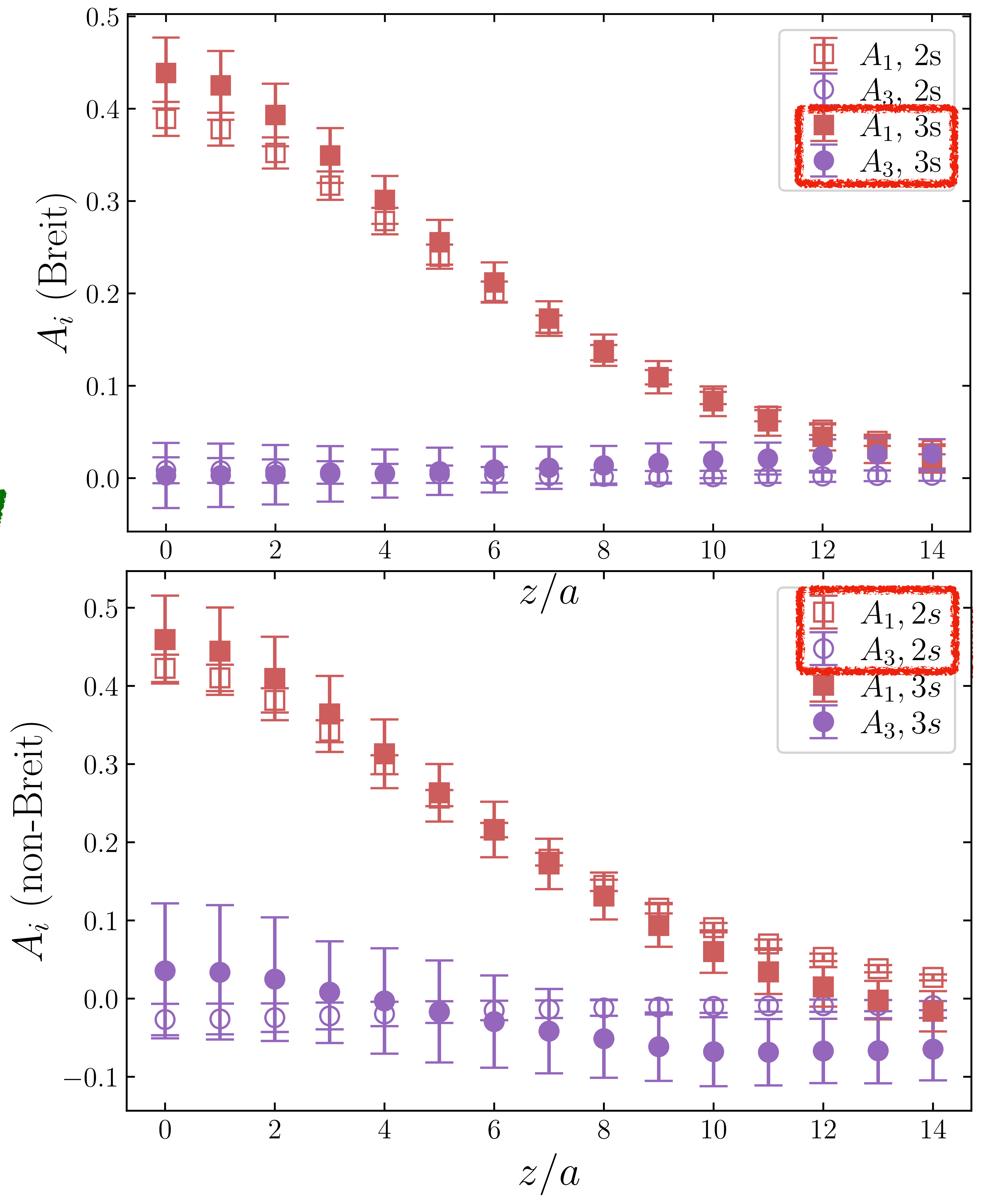

Lorentz-invariant Amplitudes

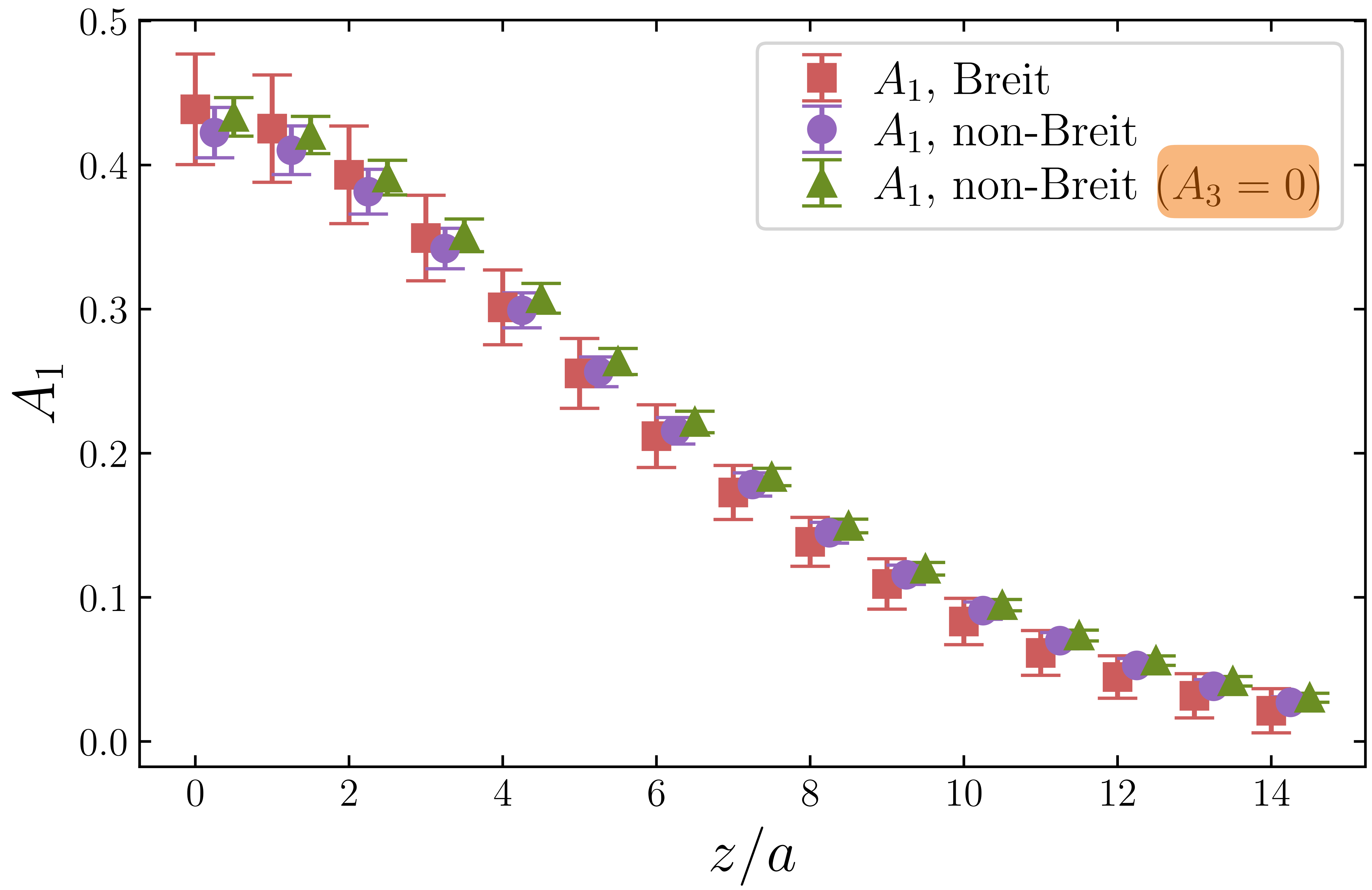

$$\widetilde{H}_{\mathrm{LI}}(zP_z, -t, z^2) = A_1(zP_z, -t, z^2) \xrightarrow{M \equiv M/\bar{P}} M(zP_z, -t, z^2)$$

Bare Matrix elements

- Largest momentum: $P_z = 1.937\ \mathrm{GeV}$,
- Varying different momentum transfer $-t$

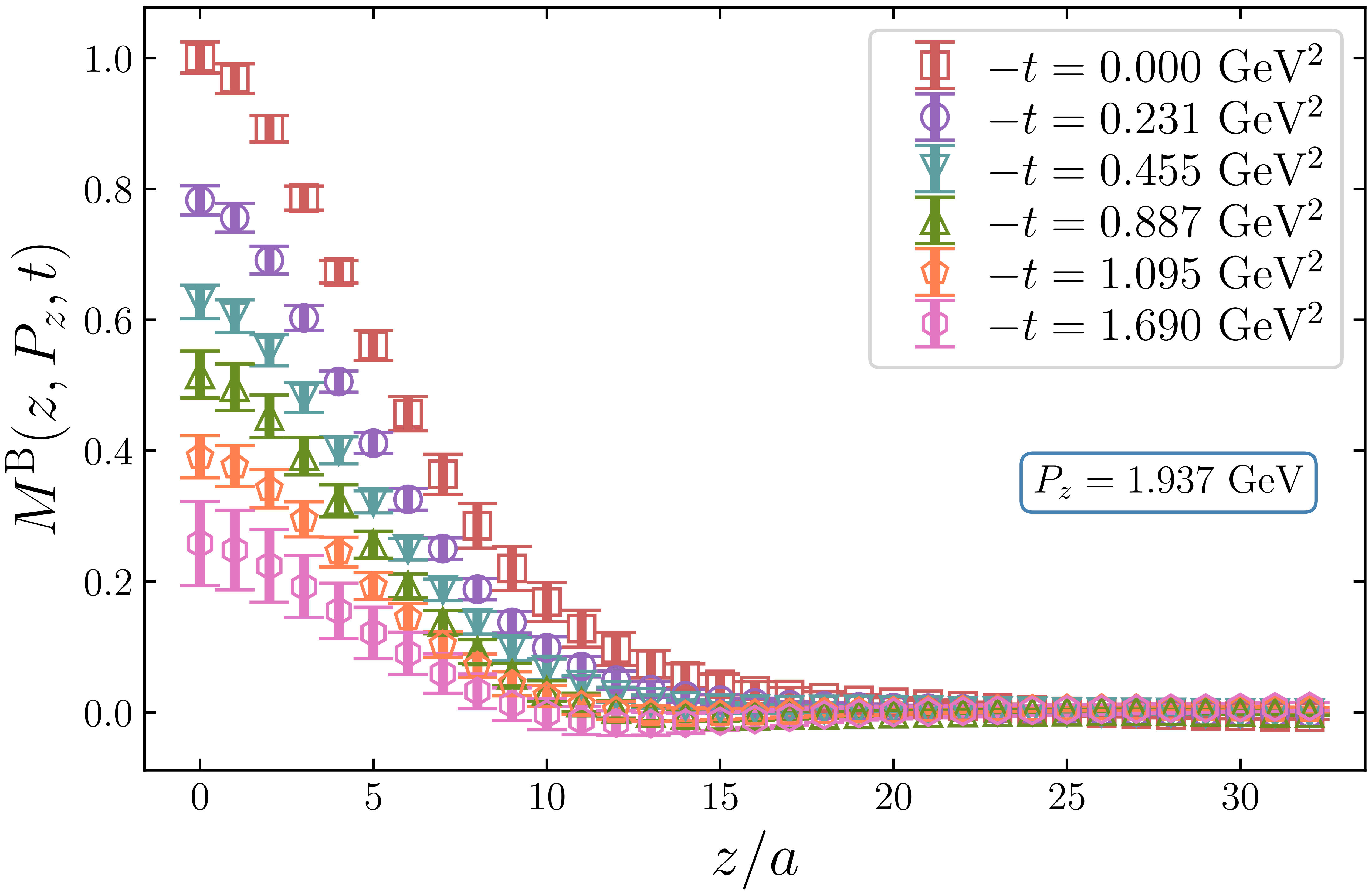

Renormalization

→

Fourier Transform

Quasi-GPDs

Renormalization: Hybrid scheme

- RI/MOM, ratio schemes — short distance

Ji et al., NPB 964 (2021) 115311

- Hybrid scheme — short & long distance

Logarithmic **Address the scheme dependence**

$$M^{\mathrm{B}}(z,a) = Z(a) e^{-\delta m(a)|z|} e^{-\bar{m}_0|z|} M^{\mathrm{R}}(z)\,.$$

Linear

Gao et al., PRL 128 (2022) 142003

$$\text{Hybrid scheme, } M^{\mathrm{R}}(z, z_s; P_z, t) = \begin{cases} |z| \le |z_S| : & \dfrac{M^{\mathrm{B}}(z, P_z, t)}{M^{\mathrm{B}}(z, 0, 0)}, \quad \text{Ratio scheme} \\ |z| \ge |z_S| : & \dfrac{M^{\mathrm{B}}(z, P_z, t)}{M^{\mathrm{B}}(z_S, 0, 0)} e^{(\delta m + \bar{m}_0)|z - z_S|}\,. \end{cases}$$

$$M^{\bar{\mathrm{R}}}(z, z_s; P_z, t) = M^{\mathrm{R}}(z, z_s; P_z, t)/F(P_z, t), \quad F(P_z, t) \equiv M^{\mathrm{B}}(0, P_z, t)/M^{\mathrm{B}}(0,0,0)\,.$$

Hybrid-scheme

Gao et al., PRL 128 (2022) 142003

- δm: $a\delta m(a) = 0.1508(12)$ for $a = 0.04$ fm lattice.
- $\bar{m}_0$: $M^{\rm B}$ at $P_z = 0$ GeV, $t = 0$ GeV^2;

$$e^{(\delta m+\bar{m}_0)\delta z}\frac{M^{\rm B}(z+\delta z)}{M^{\rm B}(z)} = \frac{C_0(\alpha_s(\mu_0(z+\delta z)), \mu_0^2(z+\delta z)^2)}{C_0(\alpha_s(\mu_0(z)), \mu_0^2 z^2)} \exp\left[\int_{\alpha_s(\mu_0(z+\delta z))}^{\alpha_s(\mu_0(z))} \frac{d\alpha_s(\mu')}{\beta[\alpha_s(\mu')]}\gamma_O[\alpha_s(\mu')]\right].$$

Leading-Renormalon Resummation

- **NLO & NNLO + LRR ($\mu = 2$ GeV)**

Renormalization Group Resummation

- **NLO & NNLO + LRR + RGR**

$\mu_0 = 2\kappa e^{-\gamma_E}/z \to \mu = 2$ GeV

$\kappa = [1, 1.414, 2]$

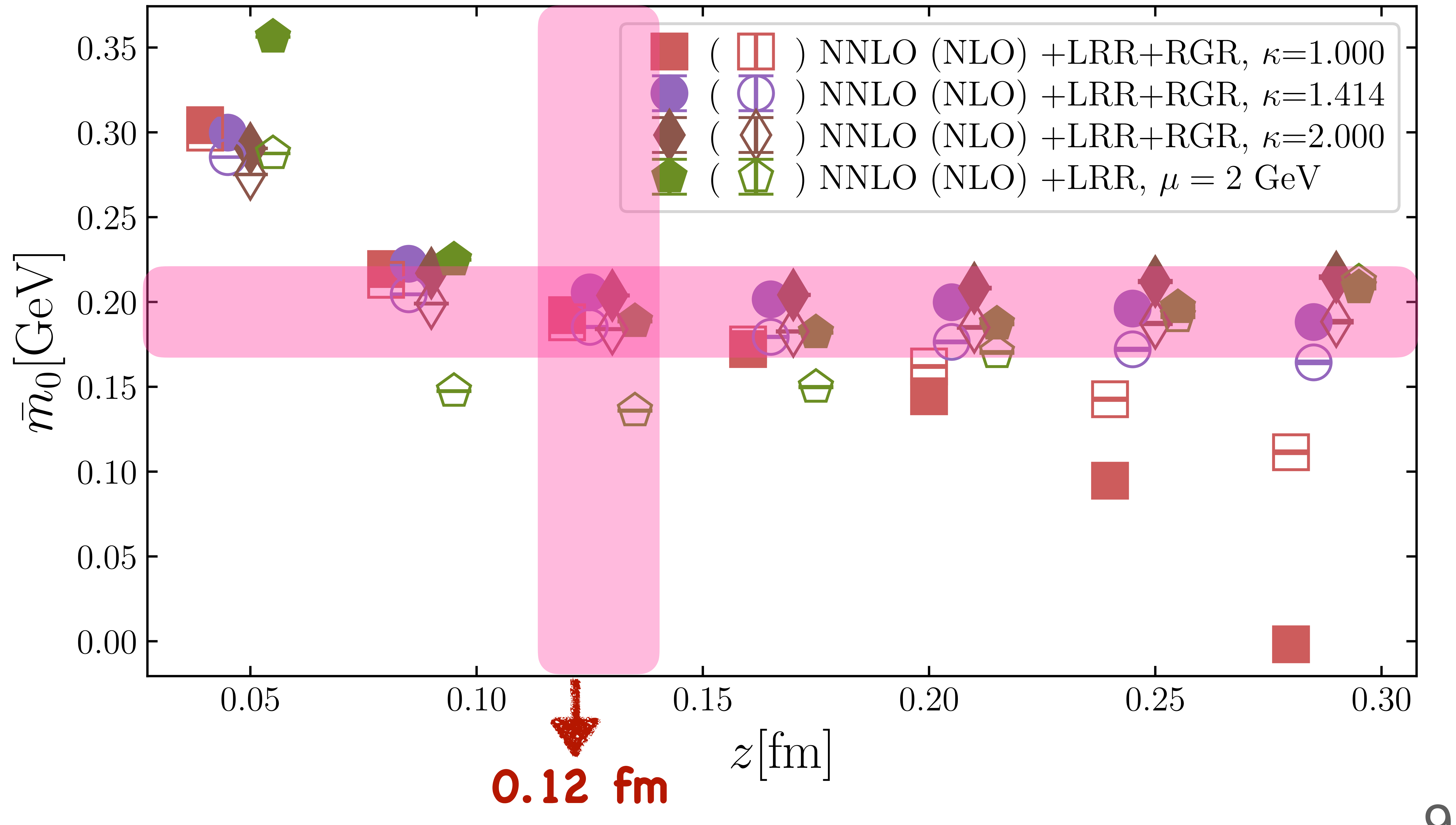

Renormalization & Extrapolation

Lattice artifacts

↓

Unphysical oscillations in quasi-GPDs

↓

Extrapolation

$$M^{\bar{R}} = A\frac{e^{-mz}}{\lambda^d}$$

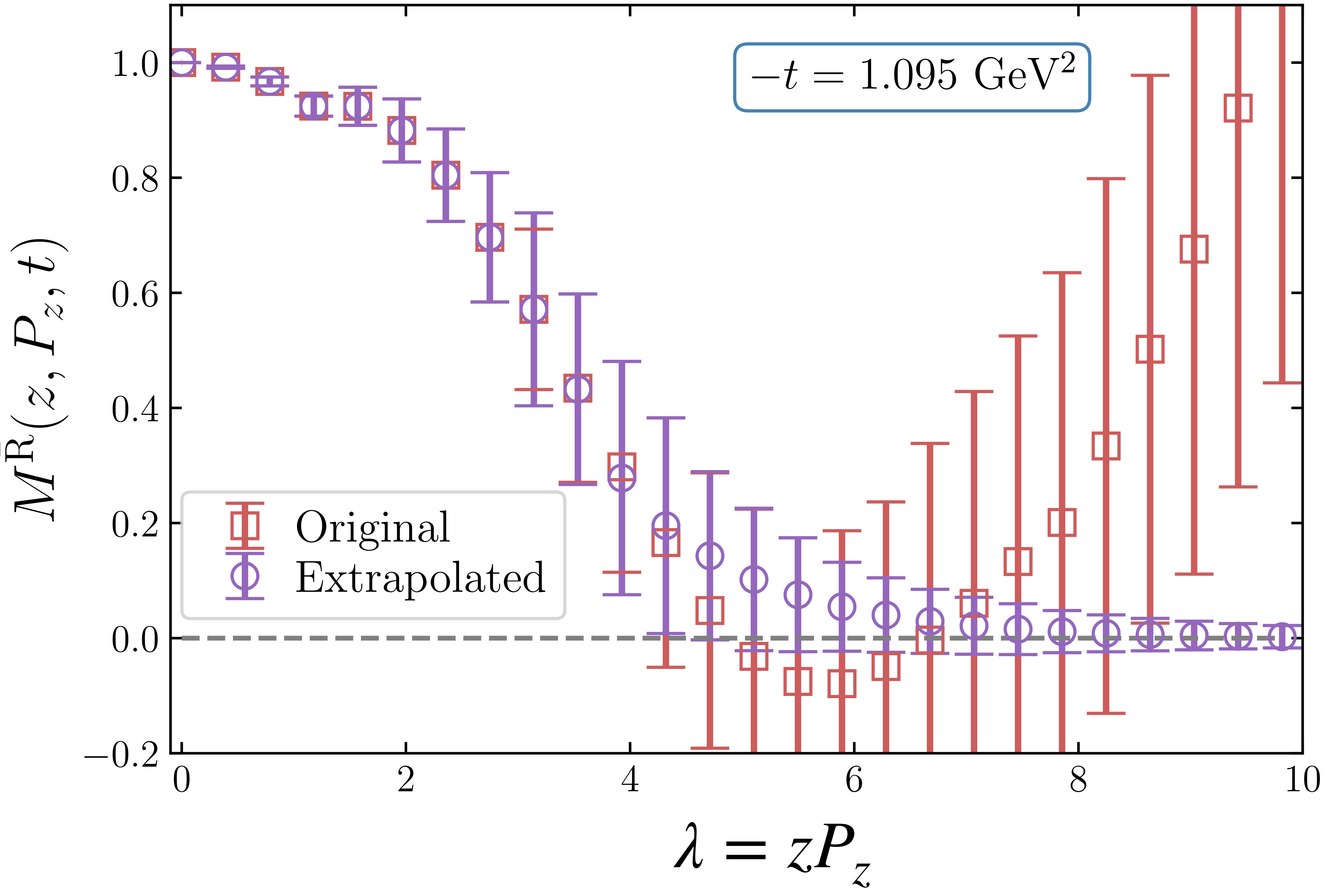

Quasi-GPDs

$$\widetilde{H}(x, P_z, t) = 2\int_{-\infty}^{\infty} \frac{d\lambda}{2\pi} e^{ix\lambda} \widetilde{H}_{\rm LI}(zP_z, t, z^2) = F(P_z, t) \int_{-\infty}^{\infty} \frac{d\lambda}{\pi} e^{ix\lambda} M^{\bar{\rm R}}(z, P_z, t)$$

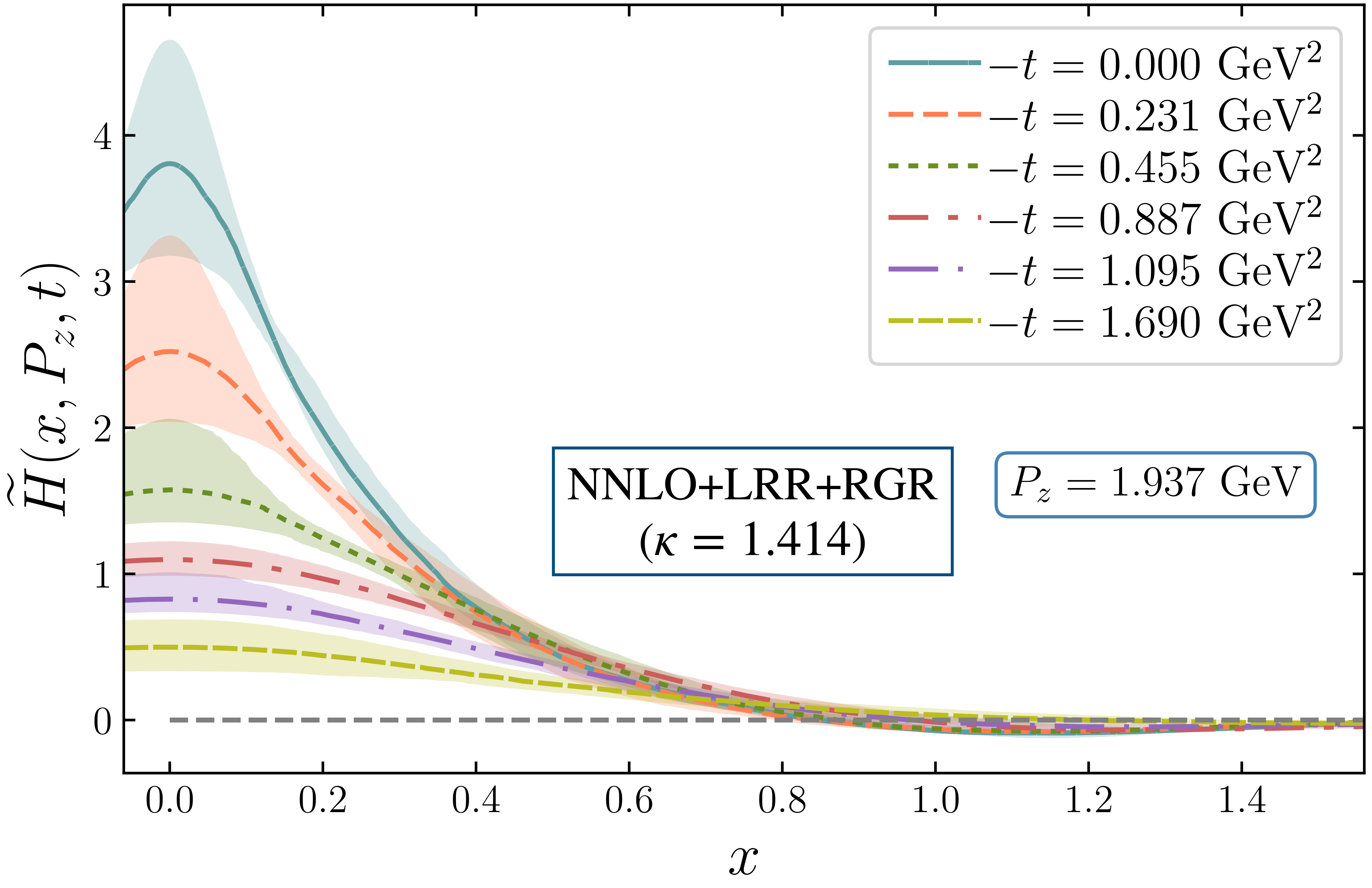

$-t$ increases

Smaller, decay slower

Light-cone GPDs

$$H(x,\mu,t) = \int_{-\infty}^{\infty} \frac{\mathrm{d}k}{|k|} \int_{-\infty}^{\infty} \frac{\mathrm{d}y}{|y|} \mathscr{C}_{\text{evo}}^{-1}\left(\frac{x}{k}, \frac{\mu}{\mu_0}\right) \mathscr{C}^{-1}\left(\frac{k}{y}, \frac{\mu_0}{yP_z}, |y|\lambda_s\right) \widetilde{H}(y, P_z, t, z_s, \mu_0)$$

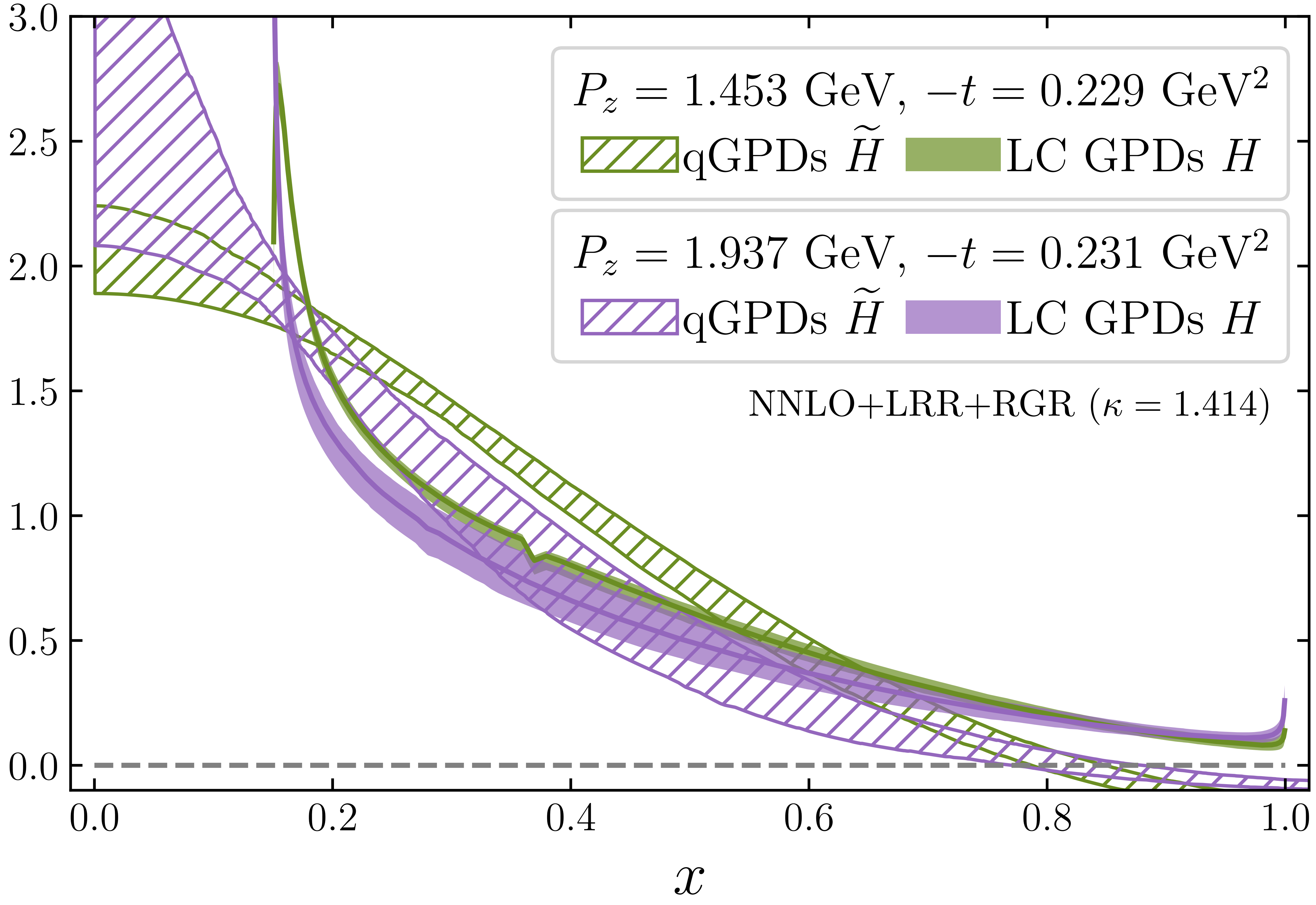

- Perturbative matching:
  - More significant at small and large x
  - Reduce the P_z-dependence

Light-cone GPDs

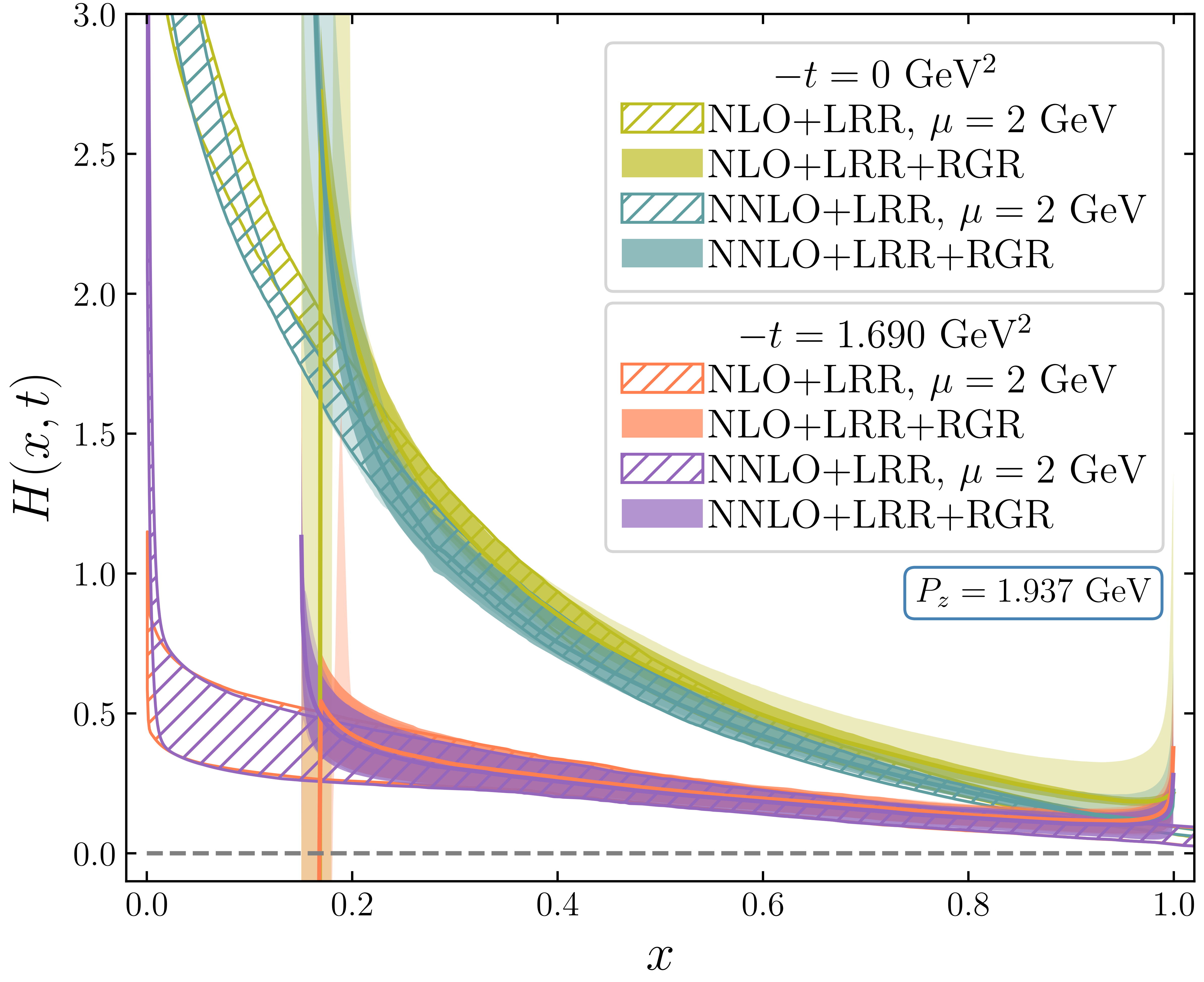

- Scale variation
  - More significant at small and large x
  - Smaller at higher order
  - Smaller at larger $-t$
- Good convergence

Light-cone GPDs

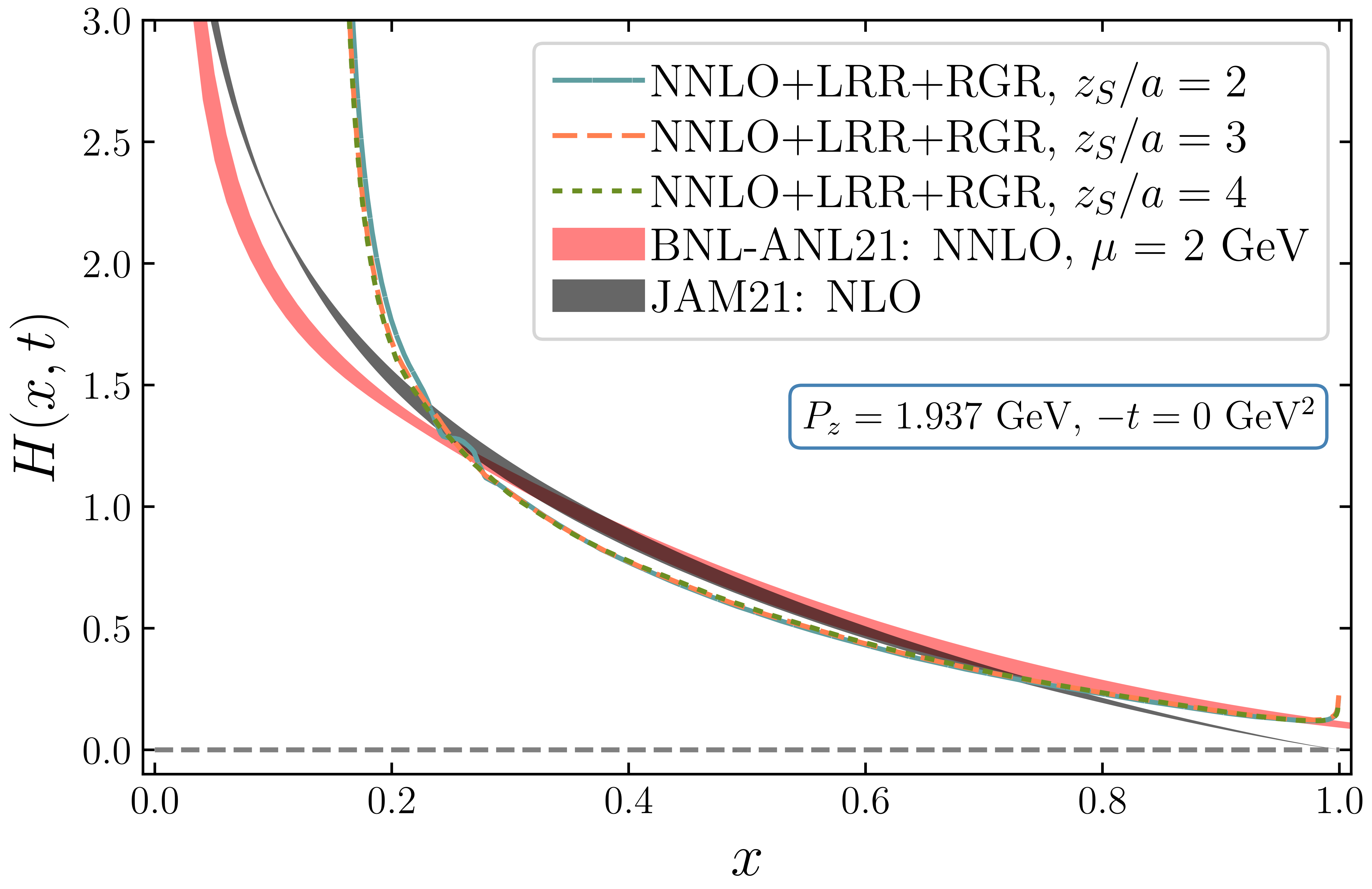

- Rare z_s dependence
- GPDs at $-t$ = 0 GeV^2 —— PDFs agree well with BNL-ANL21 and JAM21

Light-cone GPDs: t-dependence

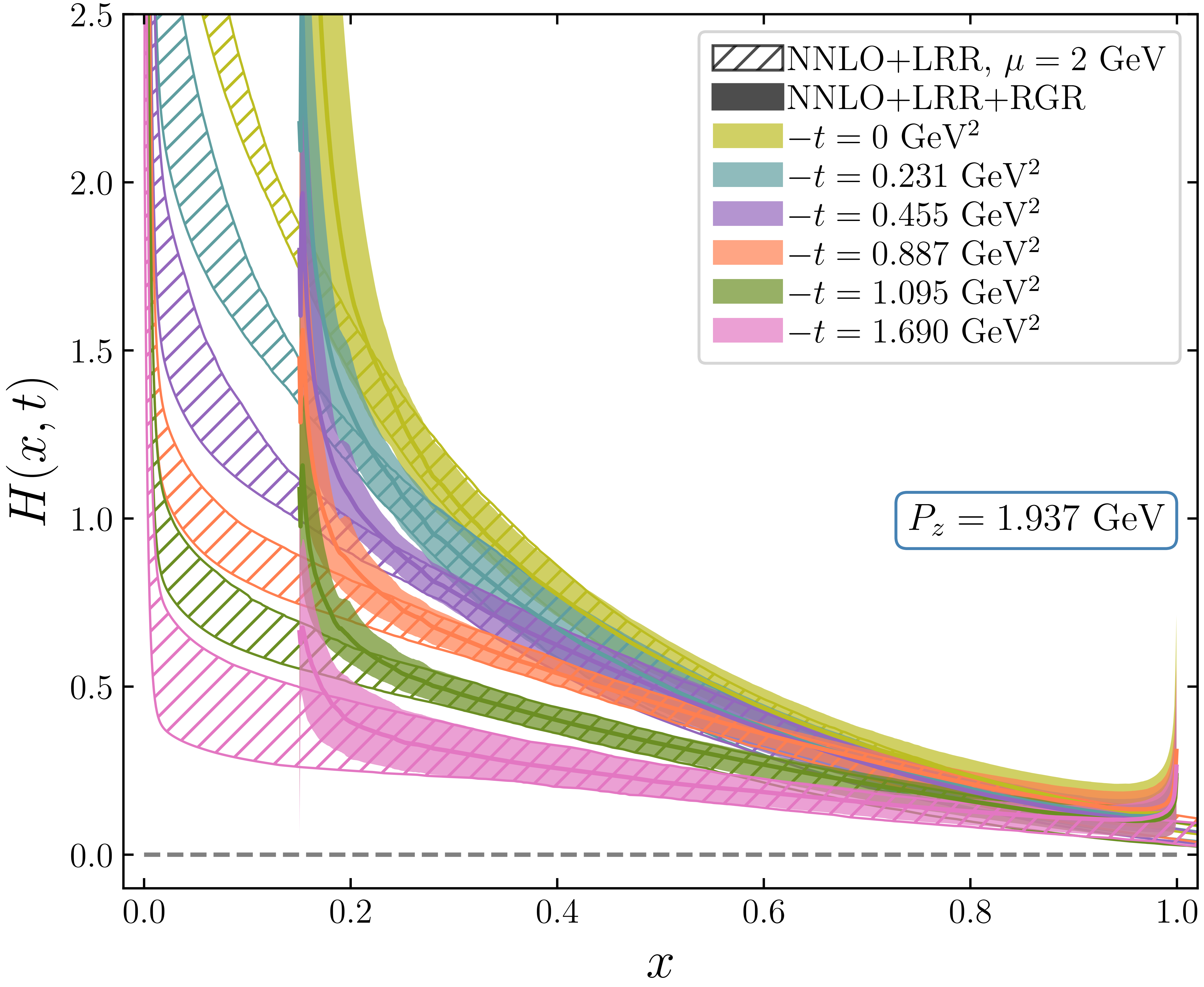

- At fixed x, H decreases as $-t$ increases
- The decrease of H along x is slower at larger $-t$
- RGR: perturbative theory breaks down at small x

Light-cone GPDs

$$H(x,t) = \frac{H(x,0)}{1 - t/M^2(x)}$$

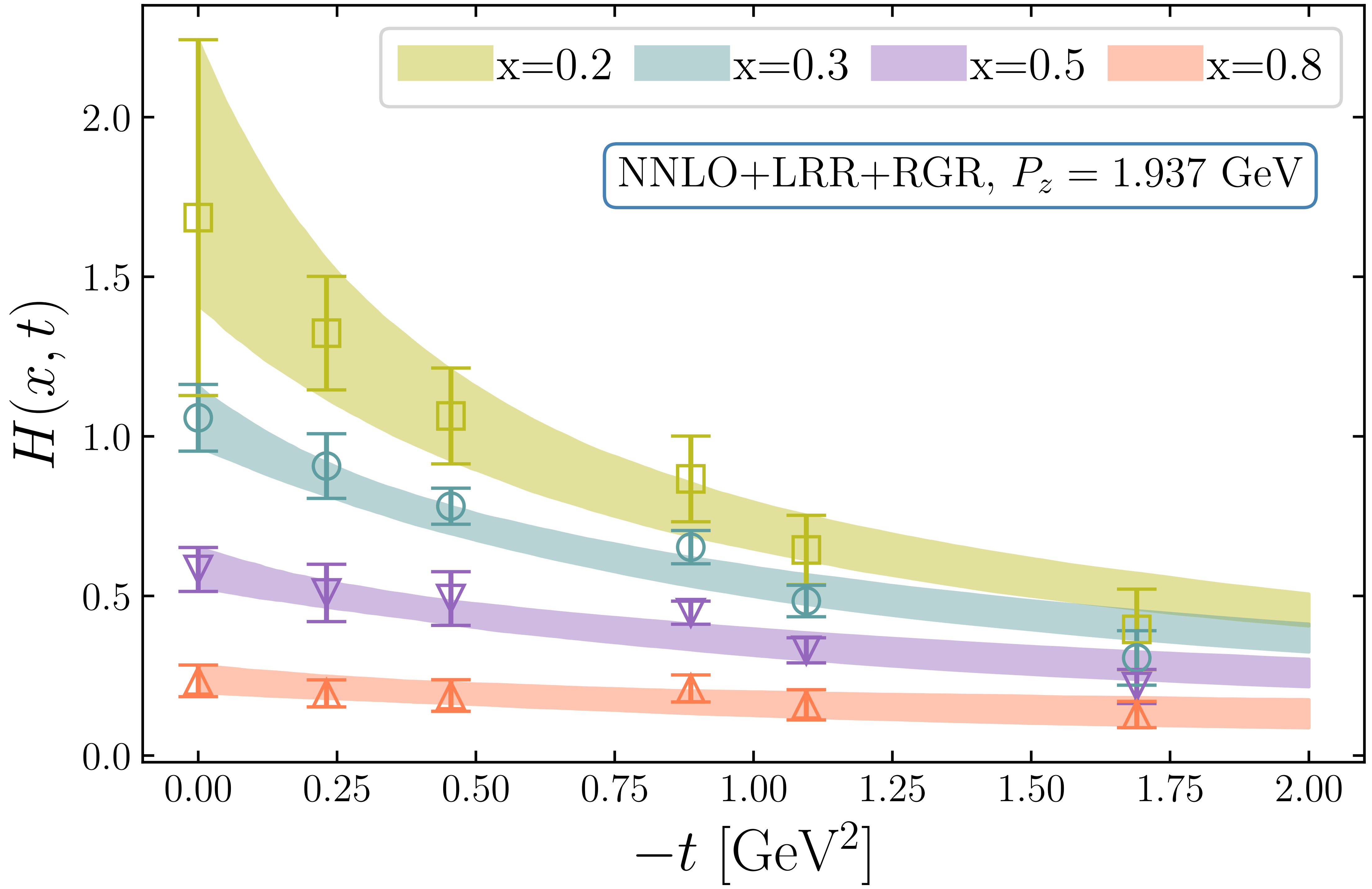

t-dependence becomes milder as x increases

Pion effective radius $\langle r^2(x)\rangle = 6/M^2(x)$

Gao et al., PRD 104 (2021) 114515

$\sim \langle r_\pi^2 \rangle = 0.313(27)$ fm^2

charge radius obtained from the EMFF

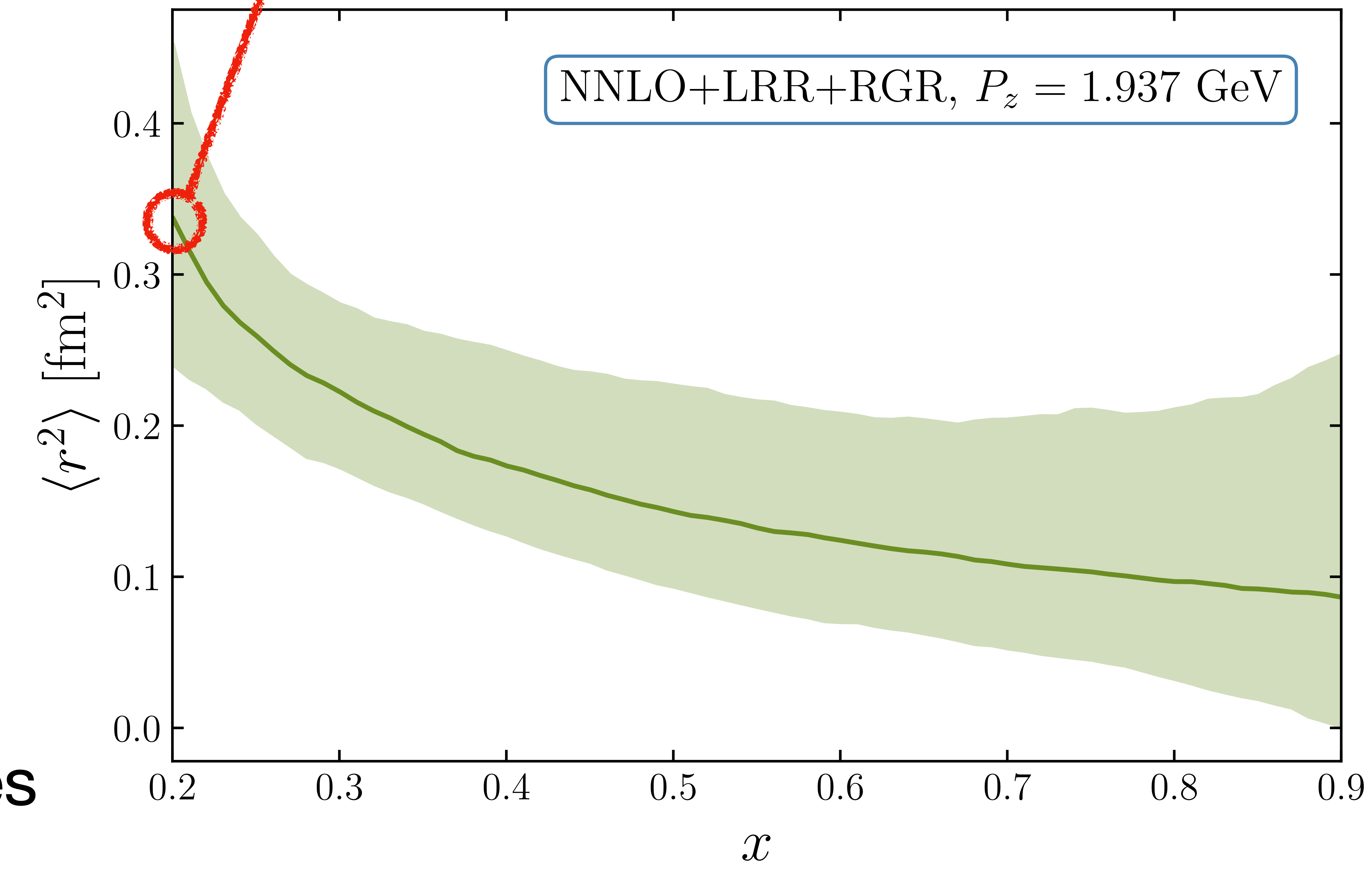

Impact-parameter-space parton distributions (IPDs)

$$q(x, \mathbf{b}_\perp) = \int \frac{d^2\mathbf{\Delta}_\perp}{(2\pi)^2} H(x, \xi = 0, \mathbf{\Delta}_\perp^2) e^{i\mathbf{b}_\perp \cdot \mathbf{\Delta}_\perp}$$

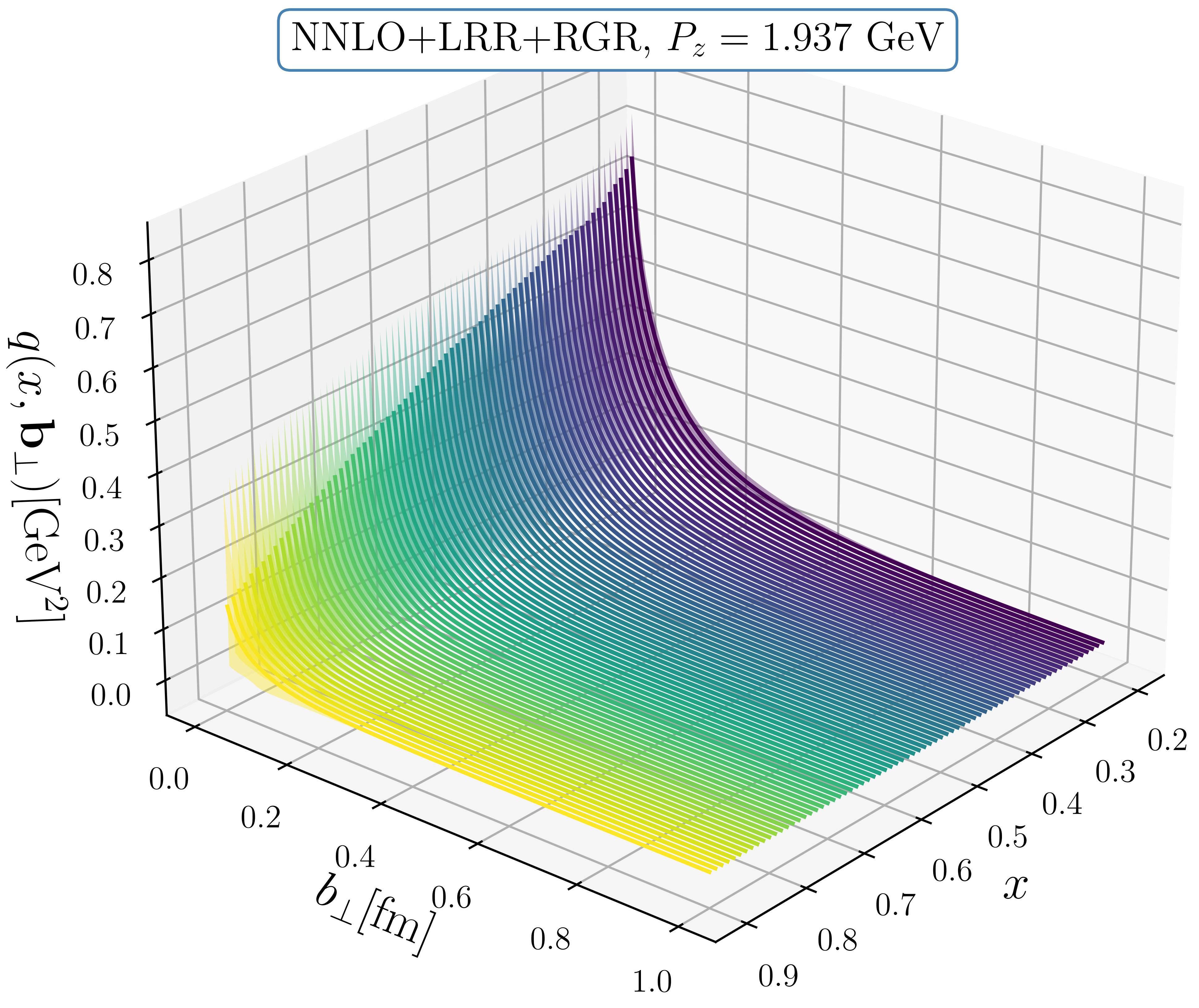

Quarks with higher x are more concentrated

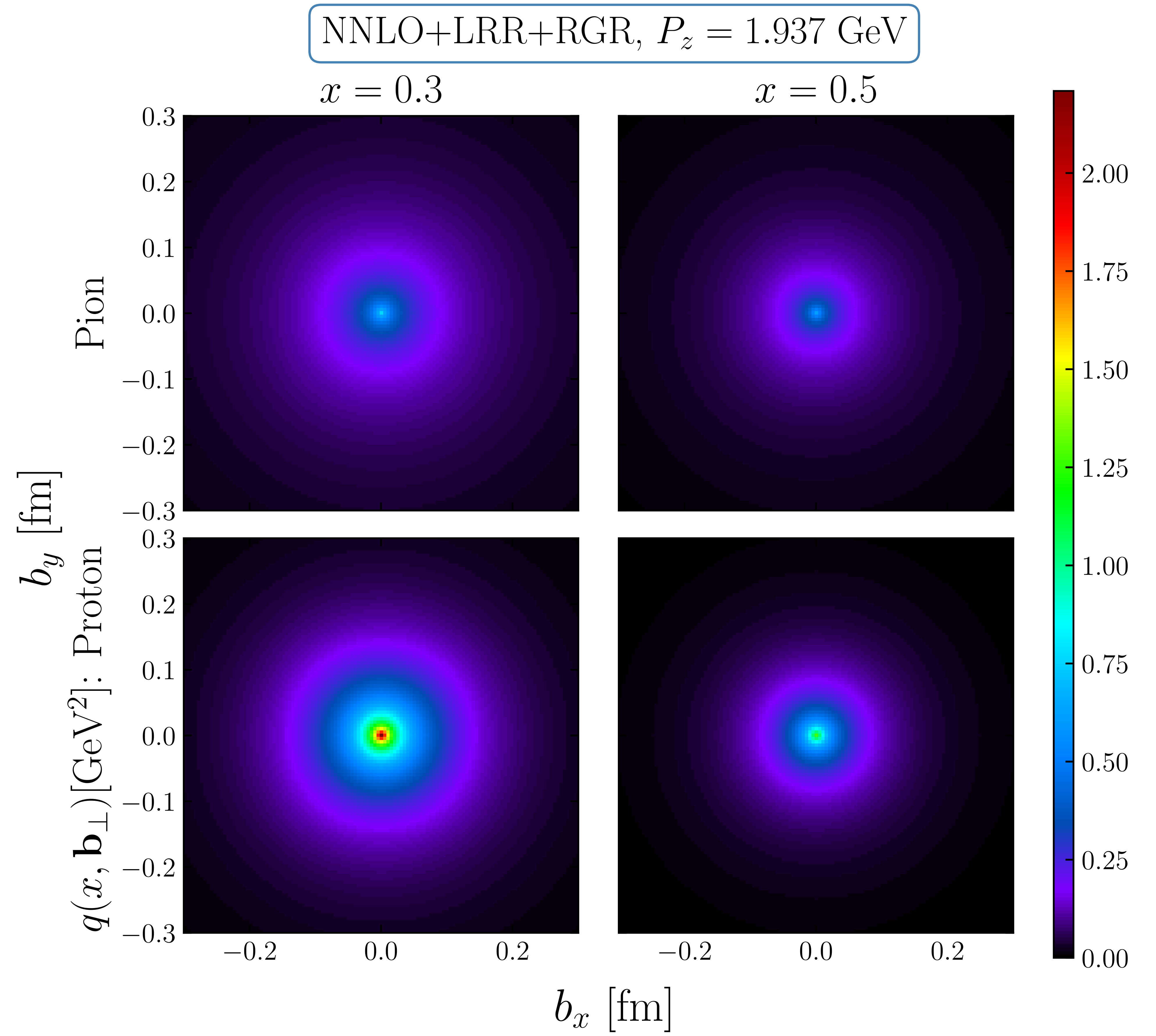

LC Proton GPDs: Cichy et al., arXiv:2304.14970

- Distributions are more concentrated at larger x
- Proton is more broader than pion

Summary

Study the pion light-cone GPDs at $\xi = 0$ using LaMET at $a = 0.04$ fm lattice

- Utilize the Lorentz-invariant definition of the GPDs
- - hybrid-scheme renormalization

  - NNLO + LRR + RGR
- PDF results agree well with the global analyses and previous lattice results
- Perturbative matching works well
- Pion effective size is smaller than that of the proton

Thanks for your attention!

Backup

Lattice Setup

- $N_s^3 \times N_t = 64^3 \times 64, \qquad a = 0.04$ fm
- HISQ action + Wilson-Clover action $\Rightarrow m_\pi^{\text{val}} = 0.3$ GeV
- Using boost smearing to enhance the signal
- Momentum transfer $-t$: 0 ~ 1.7 GeV^2

Frame	t_s/a	$\mathbf{n}^f = (n_x^f, n_y^f, n_z^f)$	m_z	P_z[GeV]	$\mathbf{n}^\Delta = (n_x^\Delta, n_y^\Delta, n_z^\Delta)$	$-t$[GeV^2]	#cfgs	(#ex, #sl)
Breit	9,12,15,18	(1, 0, 2)	2	0.968	(2, 0, 0)	0.938	115	(1, 32)
non-Breit	9,12,15,18	(0,0,0)	0	0	(0,0,0)	0	314	(3, 96)
	9,12,15,18	(0,0,2)	2	0.968	(1,2,0)	0.952	314	(4, 128)
	9,12,15	(0,0,3)	2	1.453	[(0,0,0), (1,0,0) (1,1,0), (2,0,0) (2,1,0), (2,2,0)]	[0, 0.229, 0.446, 0.855, 1.048, 1.589]	314	(4, 128)
	9,12,15	(0,0,4)	3	1.937		[0, 0.231, 0.455, 0.887, 1.095, 1.690]	564	(4, 128)